Electronic Supplementary Material

Constructing Adjacent Phosphine Oxide Ligands Confined in Mesoporous Zr-MOFs for Uranium Capture from Acidic Medium

Wen Zhang*, [a], Xiuting Dong[a], Yingxin Mu[a], Yuxin Wang[a], Jing Chen[b]

[a] State Key Laboratory of Chemical Engineering, Tianjin Key Laboratory of Membrane Science & Desalination Technology, and School of Chemical Engineering and Technology, Tianjin University, Tianjin 300350, China

[b] Collaborative Innovation Center of Advanced Nuclear Energy Technology, Beijing Key Lab of Radioactive Waste Treatment, and Institute of Nuclear and New Energy Technology, Tsinghua University, Beijing 100084, China

*To whom correspondence should be addressed. E-mail: zhang_wen@tju.edu.cn.

Number of Tables: 4; Number of Figures: 20.

Contents

1 Materials and characterizations

Dry THF was distilled from Na/benzophenone. Dimethyl vinylphosphonate was purchased from Strem Chemicals (> 95%). Diethyl phosphite was purchased from Aladdin Co., Ltd (99%). The other reagents were A.R. grade and used without further purification.

N_2 adsorption-desorption isotherms were collected on a Micromeretics Tristar II 3020 instrument at 77 K. Before the test, the MOF samples were heated at 120 ℃ under vacuum for 12 hours. Their surface areas were calculated based on the Brunauer-Emmett-Teller model (BET), and the non-local density functional theory (NLDFT) model were used to obtain their pore-size distributions.

Digested samples of MOF-808-PO and NU-1000-PO for NMR spectra were prepared as follows.[1] 2 mg MOF sample was weighed and put into a 1.5 mL vial, and then five drops of 0.1 mol/L NaOD in D_2O solution was added to the vial to digest the samples. After capping and shaking, the samples were sonicating for 60 min. In this procedure, the organic linkers and grafted 2-(diethylphosphoryl)ethyl)phosphonic acid (DEPA) were extracted into the solution, while the inorganic Zr nodes precipitated as oxides/hydroxides. For MOF-808-PO, 5.5 mL D_2O was added into the mixture, and then the mixture was centrifuged and the clear liquid supernatant was transferred to a NMR tube. For NU-1000-PO, 5.5 d_6-DMSO was added instead of D_2O for a better dissolution of HTBAPy linkers. ^{1}H NMR spectra were recorded via a bruker AVANCE IIITM HD 400 MHz spectrometer with chemical shifts reported as ppm (tetramethylsilane as the internal standard). ^{31}P NMR chemical shifts were calibrated vs. external 85% aq. H_3PO_4.

Fourier transform infrared spectra (FTIR) were recorded on a Nicolet 7600 FTIR spectrometer. Samples is mixed with dry KBr and measured under the atmosphere.

Powder X-ray diffraction patterns (PXRD) were recorded on a Bruker D8-Focus diffractometer (CuKα1 radiation, λ = 1.54056 Å).

The samples were also studied using X-ray photoelectron spectroscopy (XPS,

Thermo Fisher K-Alpha). Prior to the test, the samples were dried at 100 °C in a vacuum for 12 h.

Transmission electron micrographs (TEM) and the mapping images were taken using a JEOL JEM2100 instrument. Selected area electron diffraction images were taken by a JEM-F200 TEM at a camera length of 1500 mm.

The energy dispersive spectroscopy (EDS) analysis was taken using an Oxford Instruments with the acceleration voltage of 15 kV, and the samples were tested without coating.

2 Synthesis of (2-(diethylphosphoryl)ethyl)phosphonic acid (DEPA)

Diethylphosphine oxide (DPO). Diethylphosphine oxide was synthesized according to the Grignard reaction.[2, 3]

$$\underset{\text{H}-\overset{\overset{\displaystyle O}{\|}}{\text{P}}\text{(OEt)}_2}{} \xrightarrow{\text{EtMgBr, K}_2\text{CO}_3/\text{H}_2\text{O}} \underset{\text{H}-\overset{\overset{\displaystyle O}{\|}}{\text{P}}\text{(Et)}_2}{}$$
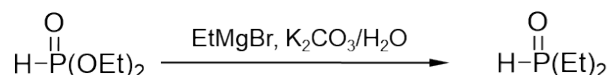
Dimethyl (2-(diethylphosphoryl)ethyl)phosphonate (DEP). This organic compound was synthesized according to the similiar reaction.[4] Specifically, 0.01 mol diethylphosphine oxide and 0.01 mol dimethyl vinylphosphonate were charged in a glass tube with 1 mL dry THF. The tube was cooled in an ice bath. Then the PMe$_3$/THF (1.0 mol/L, 5 mL) was injected into the tube using a syringe. After stirring for 30 minutes under ice bath, the tube was stirred continued for 24 h at room temperature. The THF solvent and PMe$_3$ were removed under reduce pressure.

$$(\text{MeO})_2\text{P}\diagup\!\!\diagup \; + \; \underset{\text{H}-\overset{\overset{\displaystyle O}{\|}}{\text{P}}\text{(Et)}_2}{} \xrightarrow[\text{THF, 24 h, rt}]{\text{PMe}_3 \text{ 5 mol\%}} (\text{MeO})_2\text{P}\diagdown\!\!\diagup\overset{\overset{\displaystyle O}{\|}}{\text{P}}\text{(Et)}_2$$
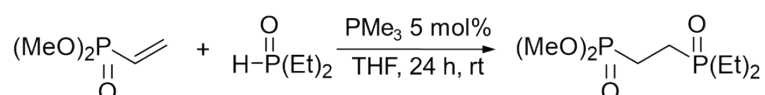
^{1}H NMR (CDCl$_3$) δ 1.03-1.15 (-CH$_3$, 6H), δ 1.70-2.03 (-CH$_2$-, 8H), δ 3.71-3.77 (-OCH$_3$, 6H). ^{31}P NMR (CDCl$_3$) δ 33.48-33.84 ((MeO)$_2$P(O)-), δ 49.05-49.40 (Et$_2$P(O)-).
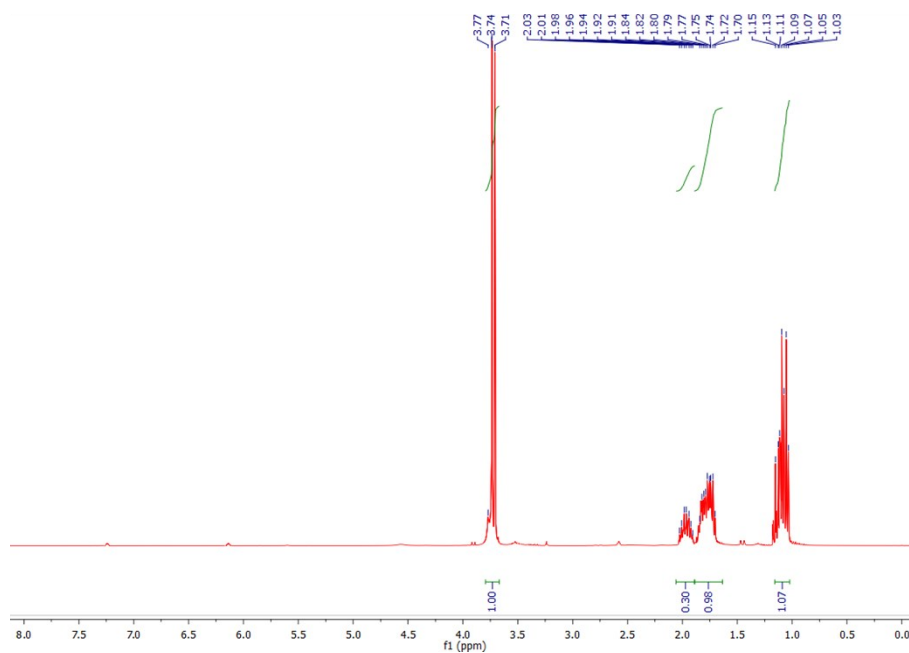
Figure S1. ^{1}H NMR of dimethyl (2-(diethylphosphoryl)ethyl)phosphonate.
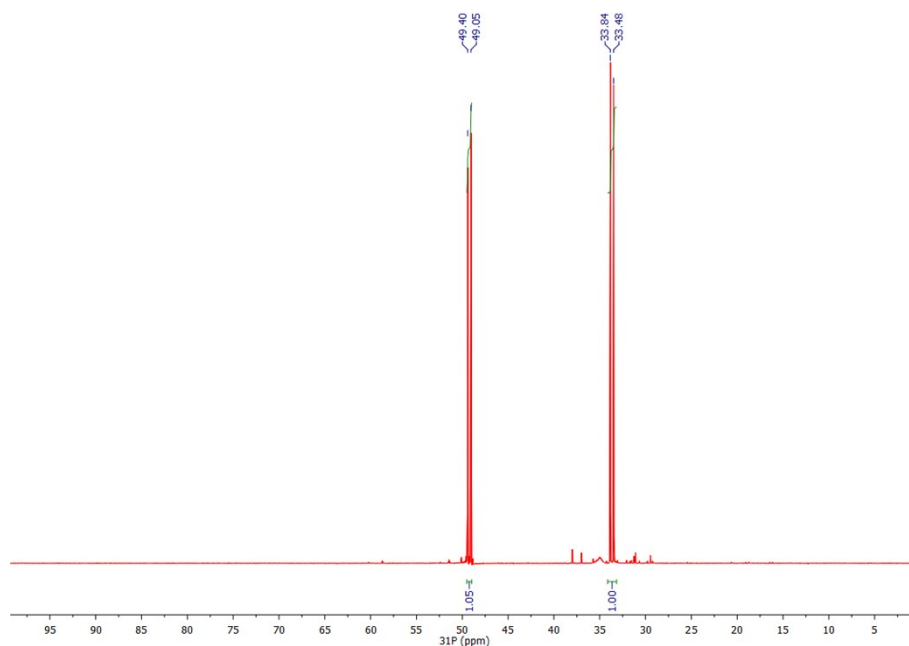
Figure S2. ^{31}P NMR of dimethyl (2-(diethylphosphoryl)ethyl)phosphonate.

(2-(diethylphosphoryl)ethyl)phosphonic acid (DEPA). 0.03 mol bromotrimethylsilane and 0.01 mol dimethyl (2-(diethylphosphoryl)ethyl)phosphonate were added into 20 mL CH_2Cl_2 under N_2 atmosphere. The mixture was then at room temperature for 24 h. The CH_2Cl_2 solvents were removed on a rotary evaporator under reduced pressure. Then 20 mL CH_3OH/CH_2Cl_2 (1:3) was added to dissolve the product.

The CH₃OH/CH₂Cl₂ solvents were removed on a rotary evaporator under reduced pressure. The residue was kept at 25°C under reduced pressure for 4 h to remove rest solvents and silylated compounds.
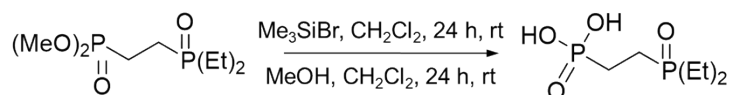
^{1}H NMR (CDCl₃) δ 0.98-1.08 (-CH₃, 6H), δ 1.57-1.93 (-CH₂-, 8H). ^{31}P NMR (CDCl₃) δ 24.74-25.06 ((HO)₂P(O)-), δ 58.79-59.11 (Et₂P(O)-).

In Figure S2, the ^{31}P NMR peak of phosphine oxide in DEP is located about 49 ppm, which is consistent with that of triethylphosphine oxide (TEPO).[5, 6] However, after the acidification of the phosphonate (DEP) to the phosphonic acid (DEPA), the ^{31}P NMR peak of phosphine oxide has shifted to 59 ppm in Figure S4, due to the hydrogen bond between the phosphine oxide groups and the hydroxyl groups on the phosphonic acids. Meanwhile, after the acidification, the ^{31}P NMR peak of phosphonate in DEP is shifted from 33 ppm to 25 ppm. The ^{31}P NMR peak of phosphonic acids in DEPA is also consistent with that of 1,2-Ethylenediphosphonic acids (26 ppm).[7, 8]
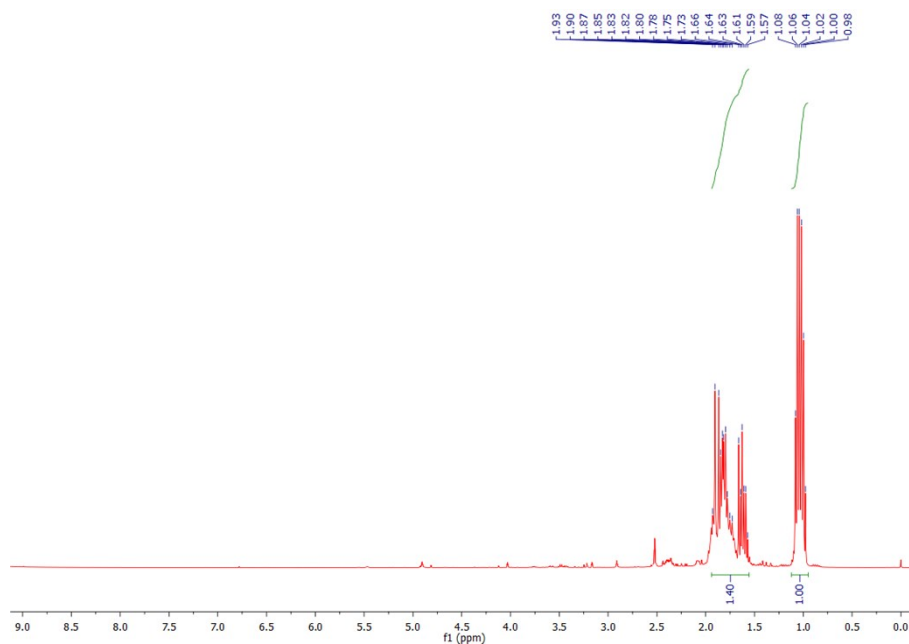
Figure S3. ^{1}H NMR of (2-(diethylphosphoryl)ethyl)phosphonic acid.
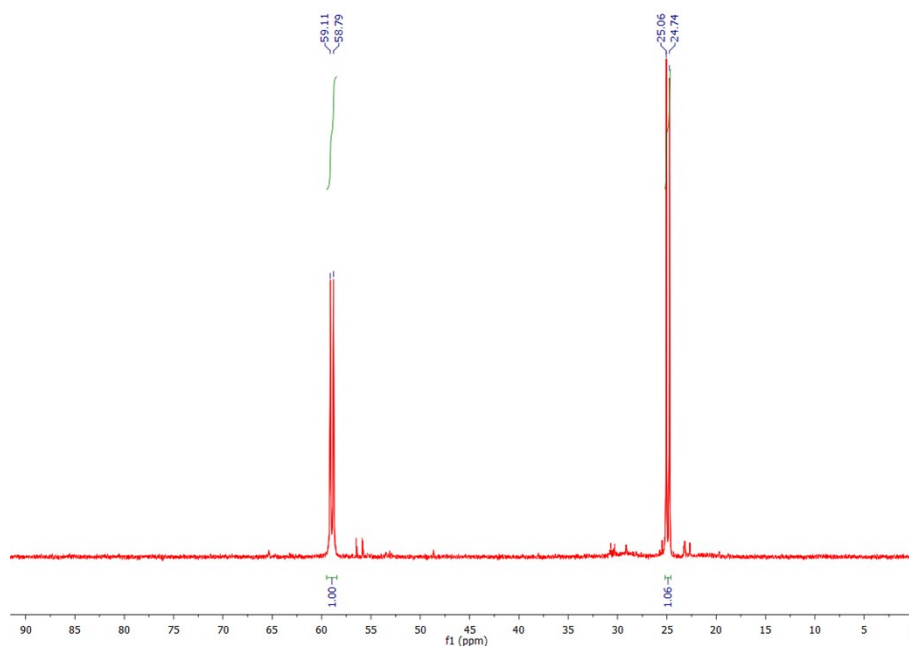
Figure S4. ^{31}P NMR of (2-(diethylphosphoryl)ethyl)phosphonic acid.

3 Synthesis of MOF-808-PO and NU-1000-PO

Synthesis of MOF-808-PO and NU-1000-PO. MOF-808 and NU-1000 was synthesized according to the literature procedures.[9, 10] 0.10 g MOF-808 or NU-1000 was soaked in 10 mL anhydrous ethanol solution with 0.2 g EDPA for 1 day under stirring at 25 ℃. After filtration, the MOF powder was washed with ethanol, deionized water and acetone for three times and then dried at 120 °C under vacuum for 1 day. After ligand exchange with EDPA, the obtained powders were denoted as MOF-808-PO or NU-1000-PO.

4 ^{1}H and ^{13}C NMR spectra of 1,3,6,8-tetrakis(p-benzoic acid)pyrene (HTBAPy)
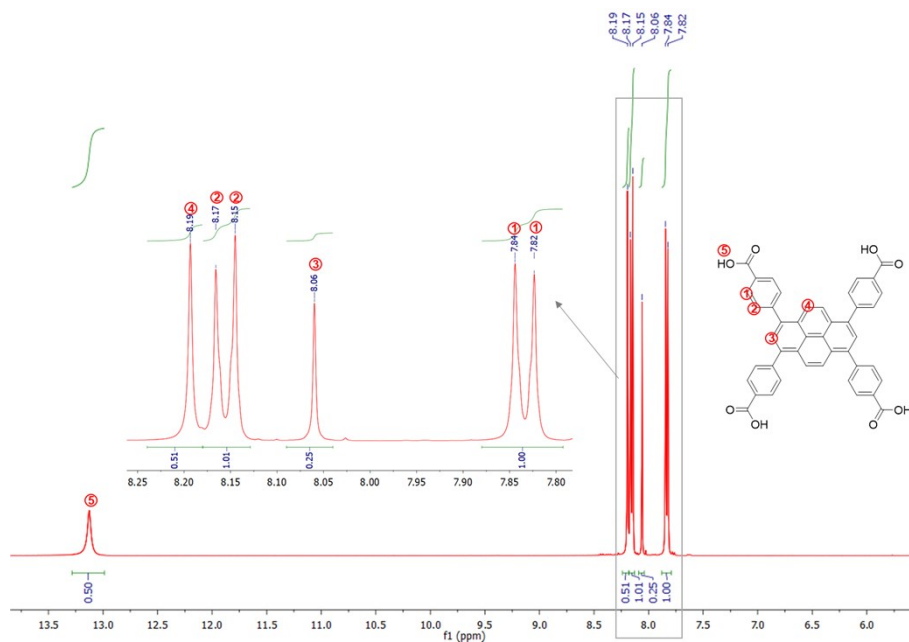
Figure S5. ^{1}H NMR of 1,3,6,8-tetrakis(p-benzoic acid)pyrene (H$_4$TBAPy)
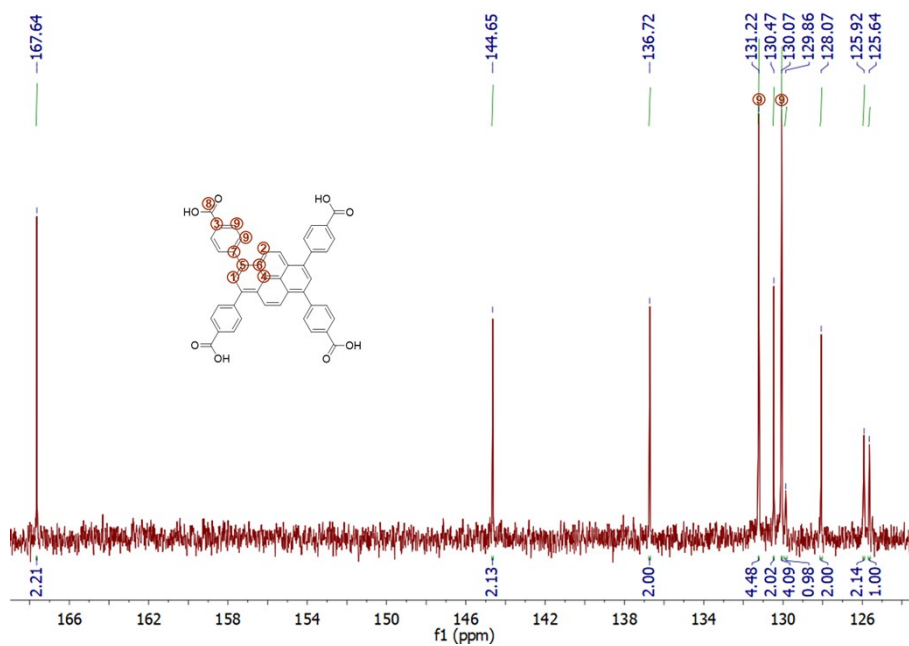
Figure S6. ^{13}C NMR of 1,3,6,8-tetrakis(p-benzoic acid)pyrene (H$_4$TBAPy)

5 ^{13}C MAS NMR spectra of MOF-808-PO and NU-1000-PO
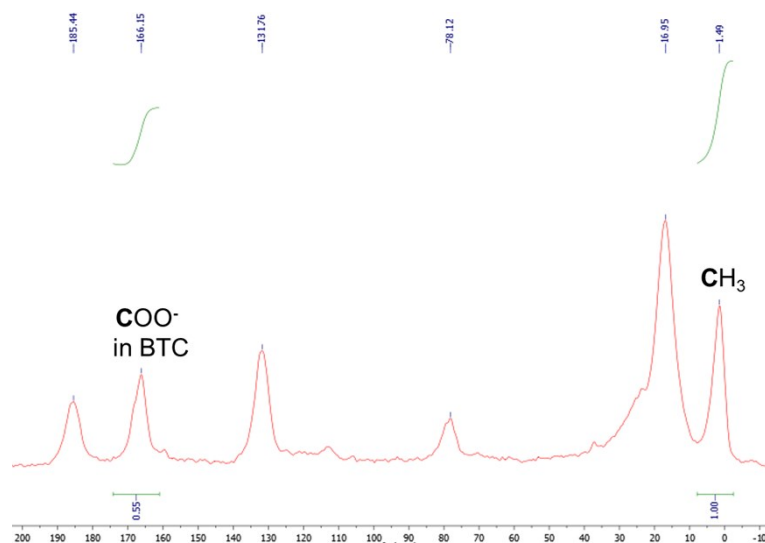
Figure S7. ^{13}C MAS NMR of MOF-808-PO.

The mole ratio of Zr-oxo nodes to BTC linkers is 1: 2, using the mole ratio of methyl groups in DEPA to carboxylate groups in BTC (1: 0.55), we could obtain the P=O groups per Zr-oxo node is 5.45.
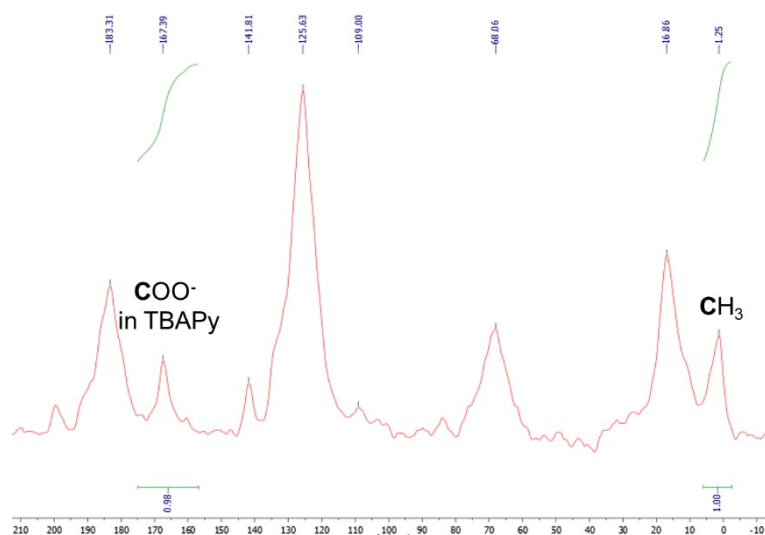
Figure S8. ^{13}C MAS NMR of NU-1000-PO.

The mole ratio of Zr-oxo nodes to TBAPy linkers is 1: 2, using the mole ratio of methyl groups in DEPA to carboxylate groups in TBAPy (1: 0.55), we could obtain the P=O groups per Zr-oxo node is 4.08.

6 EDS elemental analysis
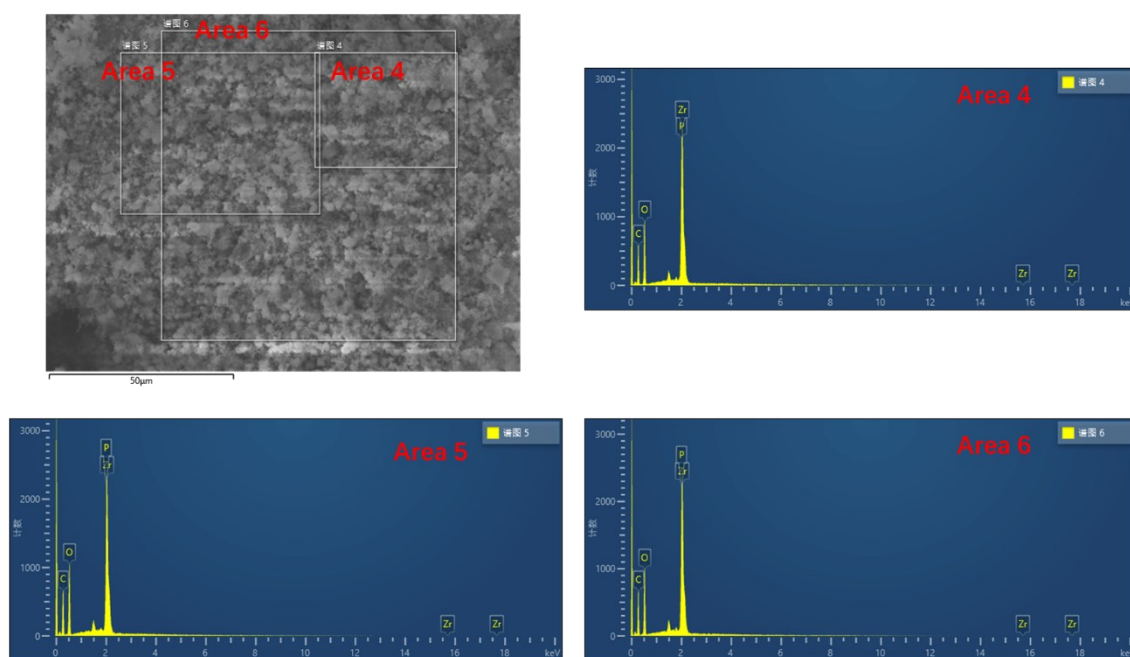
Figure S9. EDS elemental analysis of MOF-808-PO.

Table S1. EDS elemental analysis result of MOF-808-PO.

Elements	Area 4		Area 5		Area 6		Average
	Wt %	Atom %	Wt %	Atom %	Wt %	Atom %	Atom %
O	46.11	73.88	46.91	74.62	47.68	75.01	74.50
P	20.07	16.62	19.48	16.01	19.67	15.98	16.20
Zr	33.82	9.51	33.61	9.38	32.65	9.01	9.30

Using the mole ratio of P to Zr elements in MOF-808-PO (16.20: 9.30), we could obtain the P=O groups per Zr-oxo node is 5.23.
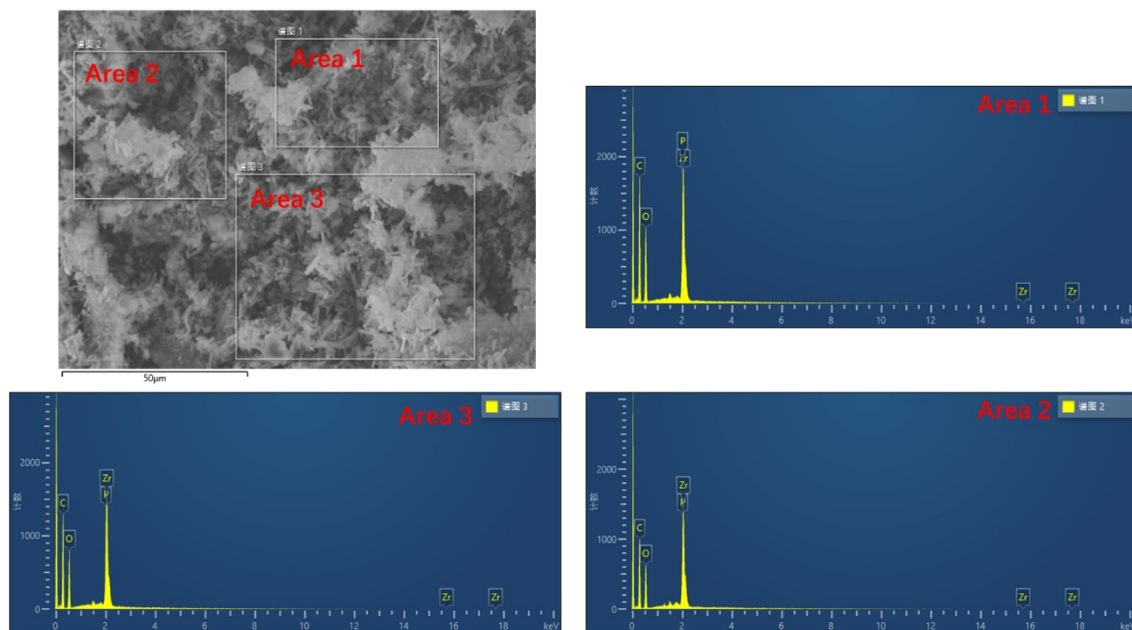
Figure S10. EDS elemental analysis of NU-1000-PO.

Table S2. EDS elemental analysis result of NU-1000-PO.

Elements	Area 1		Area 2		Area 3		Average
	Wt %	Atom %	Wt %	Atom %	Wt %	Atom %	Atom %
O	49.35	77.49	50.10	77.82	48.35	76.62	77.31
P	15.99	12.97	16.20	13.00	16.69	13.66	13.21
Zr	34.66	9.54	33.70	9.18	34.96	9.72	9.48

Using the mole ratio of P to Zr elements in NU-1000-PO (13.21: 9.48), we could obtain the P=O groups per Zr-oxo node is 4.18.

7 PXRD patterns of Zr-MOFs
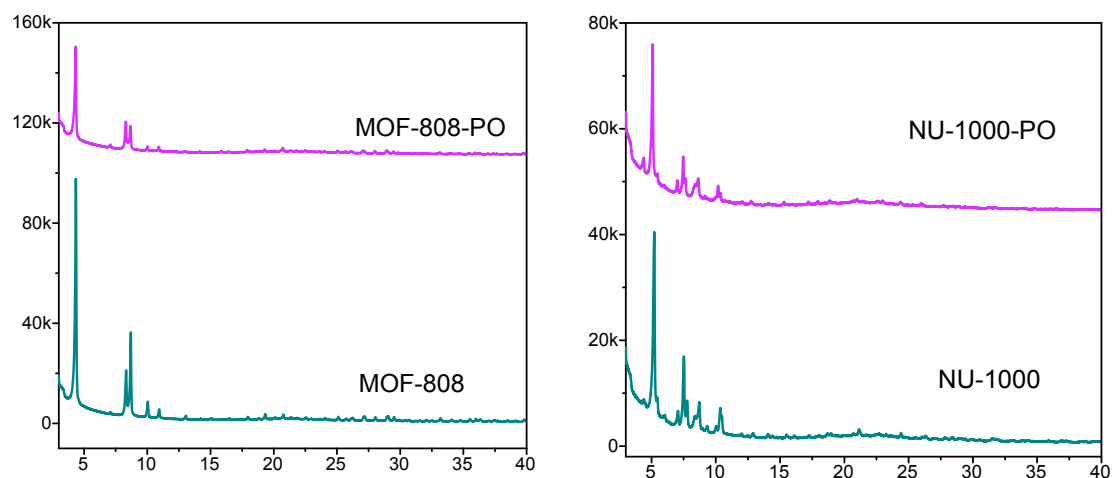
Figure S11. PXRD patterns of Zr-MOFs before and after ligand exchange.

8 Selected area electron diffraction patterns of NU-1000 and NU-1000-PO
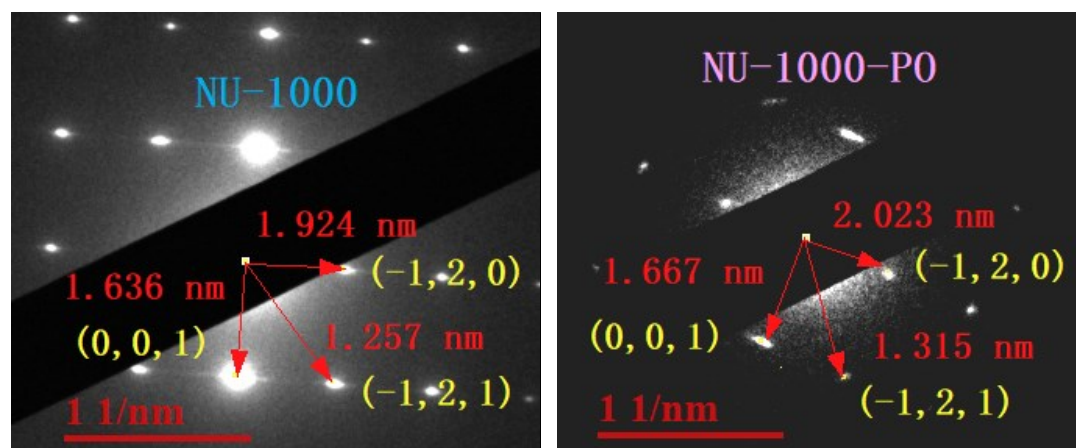
Figure S12. The selected area electron diffraction of NU-1000 and NU-1000-PO.

9 Tstransmission electron microscope (TEM) images
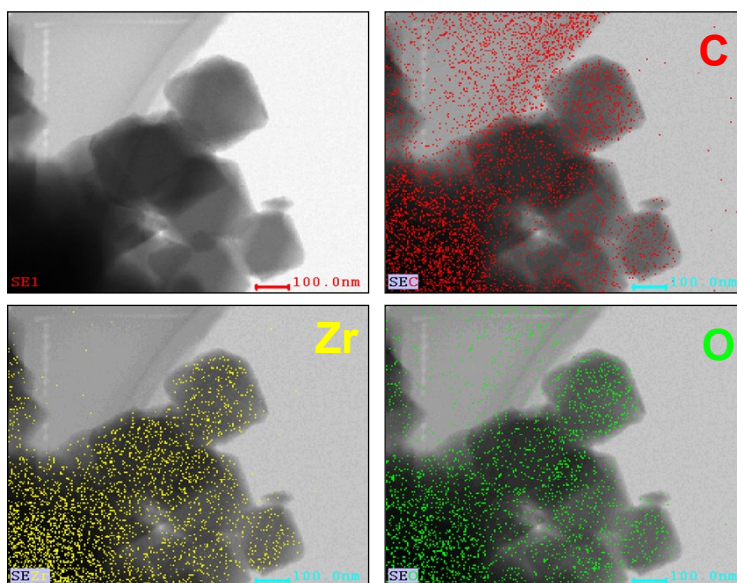
Figure S13. TEM mapping images of MOF-808.
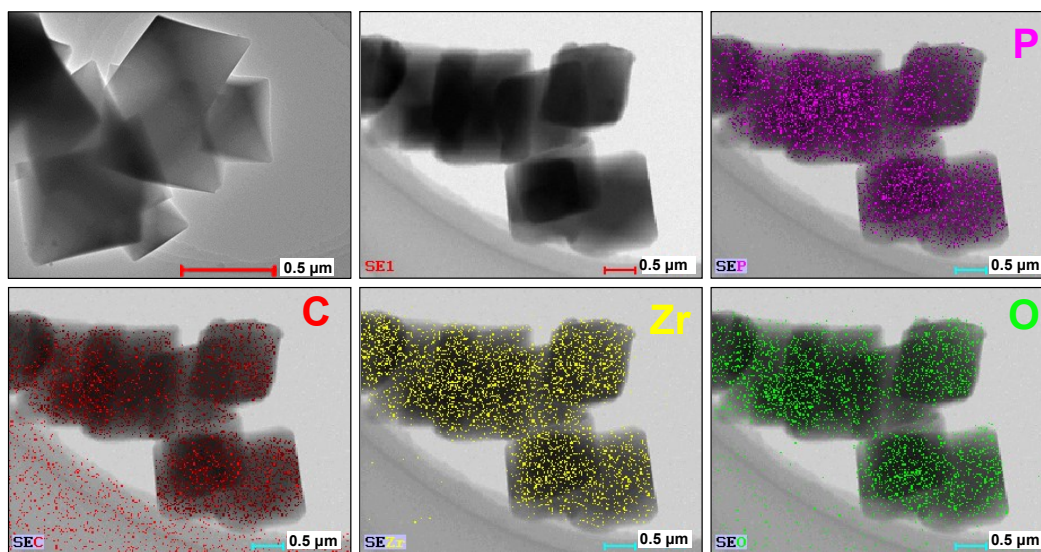
Figure S14. TEM mapping images of MOF-80-PO.
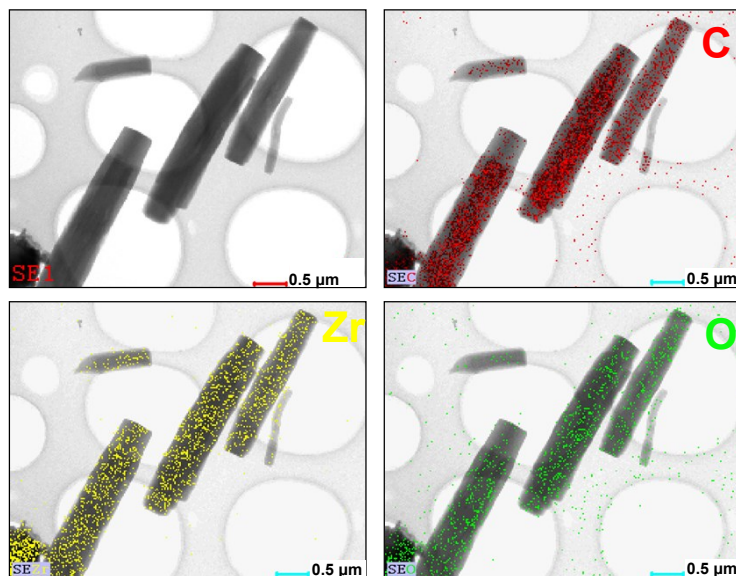
Figure S15. TEM mapping images of NU-1000.
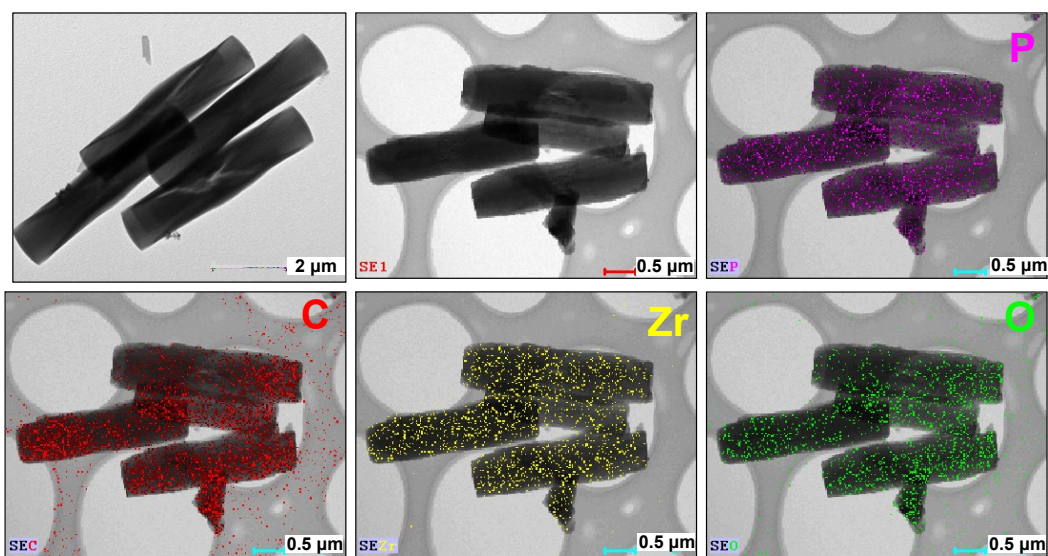
Figure S16. TEM mapping images of NU-1000-PO.

10 The stability of MOF-808-PO and NU-1000-PO in 1 mol/L HNO$_3$ solution

In the stability experiment, 10 mg of MOFs was added into 10 mL of 1 mol/L HNO$_3$ solutions for 24 hours. After filtrating using a 0.22 μm nylon syringe filter, the filter liquor was measured with ^{31}P NMR (0.5 mL filter liquor/0.5 mL D$_2$O), and the solids were measured with XRD.
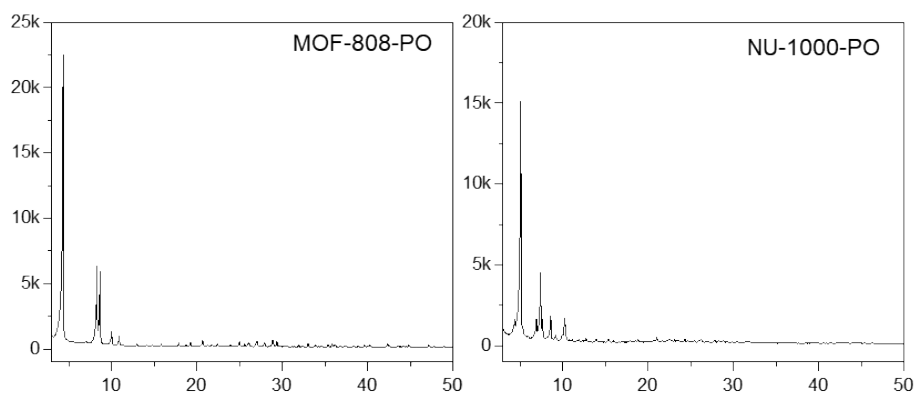
Figure S17. XRD patterns of MOFs after 1 mol/L HNO$_3$ treatment for 24 h.
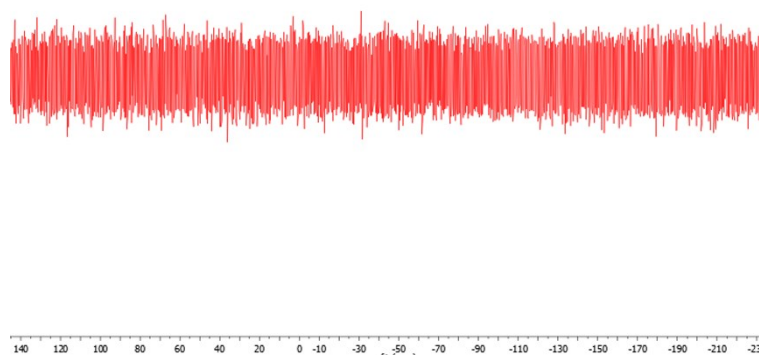
Figure S18. ^{31}P NMR of the 1 mol/L HNO$_3$ solution
after treatment of MOF-808-PO for 24 h.

140 120 100 80 60 40 20 0 -10 -30 -50 -70 -90 -110 -130 -150 -170 -190 -210 -230
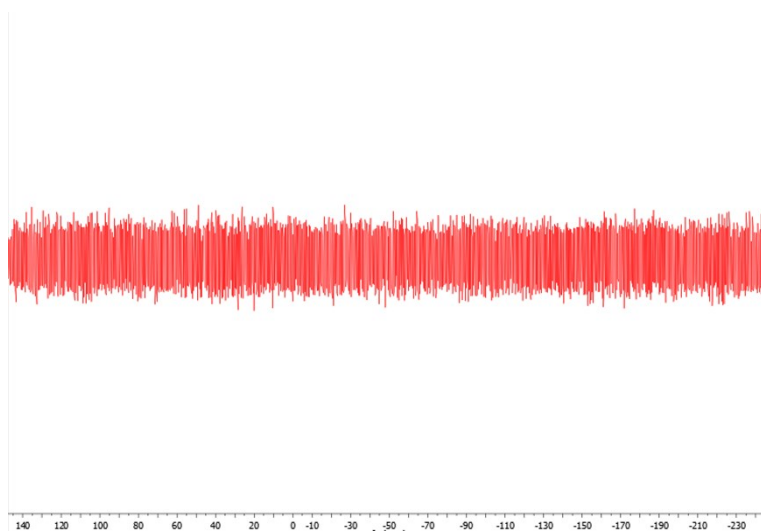
Figure S19. ^{31}P NMR of the 1 mol/L HNO$_3$ solution after treatment of NU-1000-PO for 24 h.

11 Adsorption tests

Uranium adsorption experiments were carried out at room temperature using batch tests. The initial concentration of uranium is 100 μg/mL. The initial concentrations of HNO$_3$ in the solutions are 2 mol/L, 1mol/L, 0.1 mol/L (pH=1), 0.01 mol/L (pH=2) or 0.001 mol/L (pH=3). In the adsorption experiment, 10 mg of MOFs was added into 10 mL solutions with 100 μg/mL U. The tubes were sealed and placed in a shaker with a speed of 120 rpm for 12 hours. After filtrating using a 0.22 μm nylon syringe filter, the solution was measured via the Arsenazo III spectrophotometry. The adsorption capacity (mg/g) of uranium is based on the equation,

$$Q = \frac{(C_o - C_e) \times V}{m}$$

, in which C_0 and C_e represent the uranium concentrations (ug/mL) in the solution before and after adsorption, respectively; V is the solution volume (mL), and m is the weight of the MOFs (mg) used in the adsorption test.

The adsorption ratio (AR) was calculated using the following equation.

$$AR = \frac{(C_o - C_e)}{C_o}$$

In the kinetics experiments, 5 mg MOFs were placed in 5 mL solution with 1mol/L HNO$_3$ and 100 ug/mL U(VI). Eight bottles with MOFs and solutions were prepared for the eight points in the dynamics curves.

To assess the recyclability, the desorption experiments of U(VI) adsorbed MOF-808-PO and NU-1000-PO were studied in trifluoroacetic acid (TFA) and HNO$_3$ solutions. 10 mg MOF-808-PO or NU-1000-PO was placed in 10 mL solution with 100 ug/mL U. The HNO$_3$ concentration is 1 mol/L or 0.001 mol/L(pH=3). After shaking at a speed of 120 rpm for 12 hours, the mixture was centrifuged, and the solid was washed with deionized water and dried at 80 ℃ for the next adsorption. The U(VI) adsorbed sample was immersed in a TFA/ HNO$_3$ (1 mol/L/1 mol/L) mixed elution solution and shaken at a speed of 120 rpm for 12 hours for regenerating. The uranium concentration in elution solution was measured and the elution ratio was calculated using the uranium

amount in the elution solution divided by the uranium amount adsorbed in the sample firstly. After the elution, the MOFs were used for the second adsorption.

The selectivity is tested in mixed solutions and their compositions are listed in Table S3. The concentrations of metal ions in the mixed solutions before and after adsorption were quantified by ICP-MS (Agilent 720). The solid/liquid ratio was 1 g/L in the solutions. The distribution ratio (K_d, L/g) is calculated according to the following equation,

$$K_d = \frac{(C_o - C_e) \times V}{m \times C_e}$$

, in which C_0 and C_e are the uranium concentration (ug/mL) of solution before and after adsorption, V is the volume (mL) of the solution and m is the mass of the MOFs (mg).

Table S3. Initial concentration of elements in simulated solution and the K_d values in the adsorption using MOF-808-PO and NU-1000-PO adsorbents.

Eleme-nts	Concentration of elements (ug/mL)	Salts used in solution	K_d (mL/g, pH=3)		K_d (mL/g, 1 mol/L HNO$_3$)	
			NU-1000-PO	MOF-808-PO	NU-1000-PO	MOF-808-PO
U	108	UO$_2$(NO$_3$)$_2$·6H$_2$O	—[a]	—[a]	2023.65	1166.07
Na	165	NaCl	1.21	3.04	1.82	1.21
Cr	103	CrCl$_6$·6H$_2$O	52.88	64.91	19.65	20.93
Co	128	Co(NO$_3$)$_2$·6H$_2$O	29.85	26.50	13.53	12.61
Ni	109	NiNO$_3$	46.18	45.27	21.95	19.79
Zn	103	Zn(NO$_3$)$_2$·6H$_2$O	6.39	0.30	6.94	5.40
Sr	161	SrCl·6H$_2$O	9.36	9.24	1.88	3.29
Cd	122	Cd(NO$_3$)$_2$·4H$_2$O	38.37	31.81	6.47	1.04
Cs	194	CsCl	5.21	4.97	2.96	2.64
Ba	101	BaCl$_2$·2H$_2$O	32.55	40.41	23.33	12.97
Nd	50	Nd(NO$_3$)$_3$·6H$_2$O	134.76	134.44	22.58	30.01
Sm	48	Sm(NO$_3$)$_3$·6H$_2$O	88.18	60.62	26.19	40.51
Eu	49	Eu(NO$_3$)$_3$·6H$_2$O	128.82	102.77	68.36	63.05

[a]The uranium in the solution is low than the limit of detection.

12 P 2p XPS of uranium-adsorbed Zr-MOFs from solutions
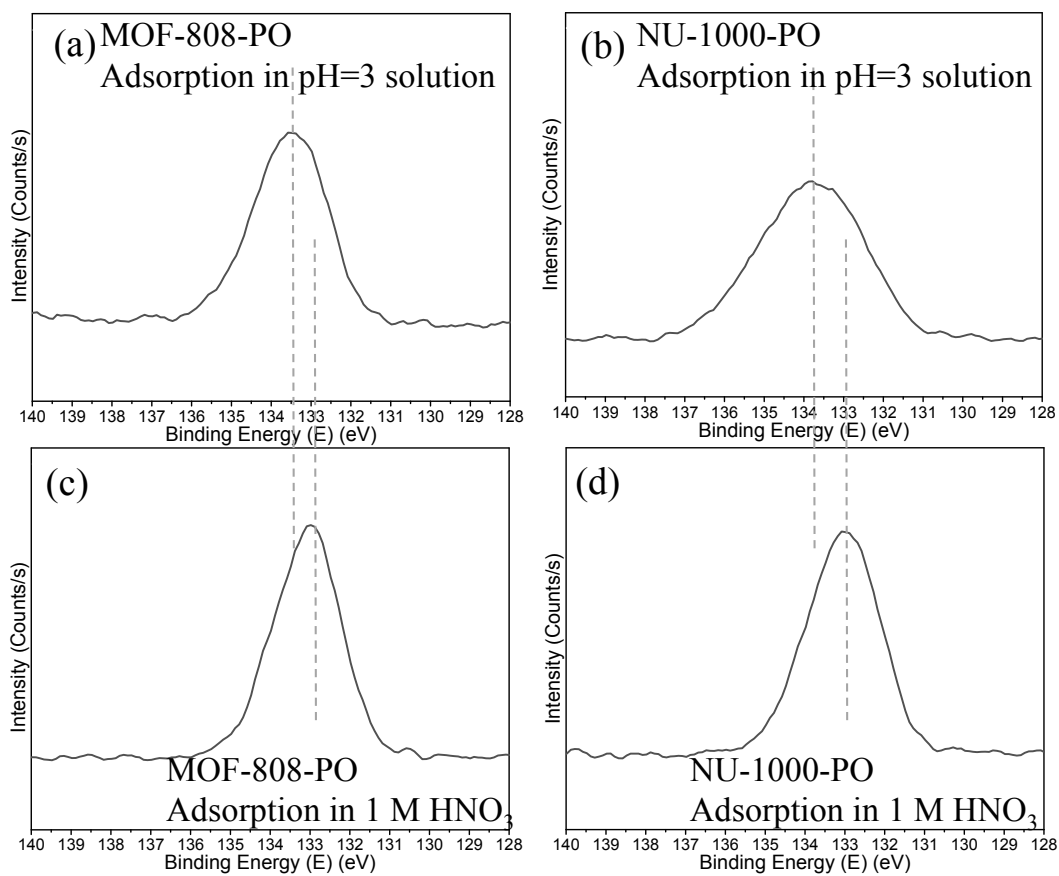
Figure S20. P 2p XPS spectra of the samples after uranium adsorption in 100 ug/mL U(VI) solution with HNO_3 concentration of 1 mol/L or 0.001 mol/L (pH=3).

13 DFT calculation methods

The density functional theory (DFT) calculations were implemented using the ORCA 4.2.0 program.[11, 12] The gas-phase geometrical optimization was carried out using the Perdew-Burke-Ernzerhof (PBE) functional[13] combinated with D3BJ dispersion correction.[14] The SDD ECP60MWB pseudopotential and basis set was employed to describe uranium (U) element,[15] and the rest elements used the def2-SV(P) basis set.[16] The calculations were accelerated by the resolution of identity (RI) technique,[17] with automatically built auxiliary basis sets. Based on the optimized structure, single point calculation was performed with the PBE0-D3BJ functional,[18] and the basis set for non-metal elements were enlarged to def2-TZVP(-f). The SMD solvation model was used for single point energies.[19] Since the rather large molecular size (> 300 atoms), no frequency calculations were performed, and only electronic energies at PBE0-D3BJ/def2-TZVP(-f)/SDD/SMD(water) level was considered.

14 The comparison of energy values for uranium complexing

Table S4. The comparison of energy values for uranium complexing reaction by phosphine ligands

Ligands (L)	Complexing products	Methods	ΔE	Refs
CMPO[a]	$[UO_2L_2]^{2+}$	DFT	−337.0 kcal/mol	[20]
OPMe$_3$	$[UO_2L_2]^{2+}$	DFT	-1047 kJ/mol	[21]
Diphenyl(2-pyridyl)phosphine oxide	$UO_2(NO_3)_2L_2$	DFT	-51.2 kcal/mol	[22]
Anchored ethylphosphine oxide	$UO_2(NO_3)_2L_2$	DFT	-59.5 kcal/mol	This work
HDDPA[b] and TOPO[c]	$UO_2(ClO_4)_2(HDDPA)_3(TOPO)$	Experiment	-78.2 kJ/mol	[23]
HDDPA and TBP[d]	$UO_2(ClO_4)_2(HDDPA)_3(TBP)$	Experiment	-77.6 kJ/mol	[23]

[a]n-octyl(phenyl)-N,N-diisobutylmethylcarbamoyl phosphine oxide;

[b]Ddodecylphosphoric acid; [c]Tri-n-octylphosphine oxide; [d]Tri-n-butyl phosphate.

References

[1] Z. Lu, J. Liu, X. Zhang, Y. Liao, R. Wang, K. Zhang, J. Lyu, O.K. Farha, J.T. Hupp, Node-Accessible Zirconium MOFs, *Journal of the American Chemical Society*, 142 (2020) 21110-21121.

[2] H.R. Hays, Reaction of diethyl phosphonate with methyl and ethyl Grignard reagents, *The Journal of Organic Chemistry*, 33 (1968) 3690-3694.

[3] C.A. Busacca, J.C. Lorenz, N. Grinberg, N. Haddad, M. Hrapchak, B. Latli, H. Lee, P. Sabila, A. Saha, M. Sarvestani, S. Shen, R. Varsolona, X. Wei, C.H. Senanayake, A Superior Method for the Reduction of Secondary Phosphine Oxides, *Organic Letters*, 7 (2005) 4277-4280.

[4] Y. Saga, D. Han, S.-i. Kawaguchi, A. Ogawa, L.-B. Han, A salt-free synthesis of 1,2-bisphosphorylethanes via an efficient PMe$_3$-catalyzed addition of >P(O)H to vinylphosphoryl compounds, *Tetrahedron Letters*, 56 (2015) 5303-5305.

[5] E. Pires, J.M. Fraile, Study of interactions between Brønsted acids and triethylphosphine oxide in solution by 31P NMR: evidence for 2 : 1 species, *Physical Chemistry Chemical Physics*, 22 (2020) 24351-24358.

[6] S. Machida, M. Sohmiya, Y. Ide, Y. Sugahara, Solid-State [31]P Nuclear Magnetic Resonance Study of Interlayer Hydroxide Surfaces of Kaolinite Probed with an Interlayer Triethylphosphine Oxide Monolayer, *Langmuir*, 34 (2018) 12694-12701.

[7] Y. Zhang, E. Oldfield, Solid-State ^{31}P NMR Chemical Shielding Tensors in Phosphonates and Bisphosphonates: A Quantum Chemical Investigation, *The Journal of Physical Chemistry B*, 108 (2004) 19533-19540.

[8] J. El Haskouri, C. Guillem, J. Latorre, A. Beltrán, D. Beltrán, P. Amorós, The First Pure Mesoporous Aluminium Phosphonates and Diphosphonates − New Hybrid Porous Materials, *European Journal of Inorganic Chemistry*, 9 (2004) 1804-1807.

[9] J. Jiang, F. Gándara, Y.-B. Zhang, K. Na, O.M. Yaghi, W.G. Klemperer, Superacidity in Sulfated Metal–Organic Framework-808, *Journal of the American Chemical Society*, 136 (2014) 12844-12847.

[10] T.C. Wang, N.A. Vermeulen, I.S. Kim, A.B.F. Martinson, J.F. Stoddart, J.T. Hupp,

O.K. Farha, Scalable synthesis and post-modification of a mesoporous metal-organic framework called NU-1000, *Nature Protocols*, 11 (2016) 149-162.

[11] F. Neese, *The ORCA program system, WIREs Computational Molecular Science*, 2 (2012) 73-78.

[12] F. Neese, *Software update: the ORCA program system, version 4.0, WIREs Computational Molecular Science*, 8 (2018) 1327.

[13] J.P. Perdew, K. Burke, M. Ernzerhof, Generalized Gradient Approximation Made Simple, *Physical Review Letters*, 77 (1996) 3865-3868.

[14] S. Grimme, J. Antony, S. Ehrlich, H. Krieg, A consistent and accurate ab initio parametrization of density functional dispersion correction (DFT-D) for the 94 elements H-Pu, *The Journal of Chemical Physics*, 132 (2010) 154104.

[15] X. Cao, M. Dolg, H. Stoll, Valence basis sets for relativistic energy-consistent small-core actinide pseudopotentials, *The Journal of Chemical Physics*, 118 (2002) 487-496.

[16] F. Weigend, R. Ahlrichs, Balanced basis sets of split valence, triple zeta valence and quadruple zeta valence quality for H to Rn: Design and assessment of accuracy, *Physical Chemistry Chemical Physics*, 7 (2005) 3297-3305.

[17] F. Neese, F. Wennmohs, A. Hansen, U. Becker, Efficient, approximate and parallel Hartree–Fock and hybrid DFT calculations. A 'chain-of-spheres' algorithm for the Hartree–Fock exchange, *Chemical Physics*, 356 (2009) 98-109.

[18] C. Adamo, V. Barone, Toward reliable density functional methods without adjustable parameters: The PBE0 model, *The Journal of Chemical Physics*, 110 (1999) 6158-6170.

[19] A.V. Marenich, C.J. Cramer, D.G. Truhlar, Universal Solvation Model Based on Solute Electron Density and on a Continuum Model of the Solvent Defined by the Bulk Dielectric Constant and Atomic Surface Tensions, *The Journal of Physical Chemistry B*, 113 (2009) 6378-6396.

[20] C. Z. Wang, J. H. Lan, Y. L. Zhao, Z. F. Chai, Y. Z. Wei, W. Q. Shi, Density Functional Theory Studies of UO_2^{2+} and NpO_2^+ Complexes with Carbamoylmethylphosphine Oxide Ligands, *Inorganic Chemistry*, 52 (2013) 196-203.

[21] C. Clavaguéra-Sarrio, S. Hoyau, N. Ismail, C.J. Marsden, Modeling Complexes of the Uranyl Ion $UO_2L_2^{n+}$: Binding Energies, Geometries, and Bonding Analysis, *The Journal of Physical Chemistry A*, 107 (2003) 4515-4525.

[22] B.G. Vats, S. Kannan, K. Parvathi, D.K. Maity, M.G.B. Drew, Steric effects in complexes of diphenyl(2-pyridyl)phosphine oxide with the uranyl ion. Synthetic, structural and theoretical studies, *Polyhedron*, 89 (2015) 116-121.

[23] M.K. Nazal, M.A. Albayyari, F.I. Khalili, E. Asoudani, Synergistic effect of tri-n-butyl phosphate (TBP) or tri-*n*-octyl phosphine oxide (TOPO) with didodecylphosphoric acid (HDDPA) on extraction of uranium(VI) and thorium(IV) ions, *Journal of Radioanalytical and Nuclear Chemistry*, 312 (2017) 133-139.